

Article

Formation and Morphology of $Zn_2Ti_3O_8$ Powders Using Hydrothermal Process without Dispersant Agent or Mineralizer

Cheng-Li Wang¹, Weng-Sing Hwang¹, Kuo-Ming Chang², Horng-Huey Ko³, Chi-Shiung Hsi⁴, Hong-Hsin Huang⁵ and Moo-Chin Wang^{3,*}

¹ Department of Materials Science and Engineering, National Cheng Kung University, 1 Ta-Hsueh Road, Tainan 70101, Taiwan; E-Mails: N58991223@ncku.edu.tw (C.-L.W.); wshwang@mail.ncku.edu.tw (W.-S.H.)

² Department of Mechanical Engineering, National Kaohsiung University of Applied Sciences, 415 Chien-Kung Road, Kaohsiung 80782, Taiwan; E-Mail: koming@cc.kuas.edu.tw

³ Department of Fragrance and Cosmetics Science, Kaohsiung Medical University, 100 Shih-Chuan 1st Road, Kaohsiung 80708, Taiwan; E-Mail: hhko@kmu.edu.tw

⁴ Department of Materials Science and Engineering, National United University, 1 Lein-Da, Kung-Ching Li, Miao-Li 36003, Taiwan; E-Mail: chsi@nuu.edu.tw

⁵ Department of Electrical Engineering, Cheng Shiu University, 840, Cheng Ching Road, Niasong, Kaohsiung 83347, Taiwan; E-Mail: funs@csu.edu.tw

* Author to whom correspondence should be addressed; E-Mail: mcwang@cc.kmu.edu.tw; Tel.: +886-7-3121101 ext. 2366; Fax: +886-7-3210683.

Received: 16 December 2010; in revised form: 18 January 2011 / Accepted: 19 January 2011 /

Published: 28 January 2011

Abstract: Synthesis of $Zn_2Ti_3O_8$ powders for attenuating UVA using $TiCl_4$, $Zn(NO_3)_2 \cdot 6H_2O$ and NH_4OH as precursor materials by hydrothermal process has been investigated. The X-ray diffractometry (XRD) results show the phases of ZnO, anatase TiO_2 and $Zn_2Ti_3O_8$ coexisted when the zinc titanate powders were calcined at 600 °C for 1 h. When calcined at 900 °C for 1 h, the XRD results reveal the existence of ZnO, Zn_2TiO_4 , rutile TiO_2 and $ZnTiO_3$. Scanning electron microscope (SEM) observations show extensive large agglomeration in the samples. Transmission electron microscope (TEM) and electron diffraction (ED) examination results indicate that $ZnTiO_3$ crystallites formed with a size of about 5 nm on the matrix of plate-like ZnO when calcined at 700 °C for 1 h. The calcination samples have acceptable absorbance at a wavelength of 400 nm, indicating that the zinc titanate precursor powders calcined at 700 °C for 1 h can be used as an UVA-attenuating agent.

Keywords: Zn₂Ti₃O₈ powders; hydrothermal; UVA-attenuating

1. Introduction

Ultraviolet (UV) radiation that reaches the earth and damages skin can be divided into three key wavelengths: (i) UVC (32–280 nm), (ii) UVB (280–320 nm) and (iii) UVA (320–400 nm). UVA radiation is a major culprit in photoaging and skin cancers. Moreover, UVB, which primarily reaches the top-most layer of skin, is thought to be responsible for acute photodamage, including sunburn and some non-melanoma skin cancers [1]. Therefore, protection against harmful UVA and UVB radiation is very important. Sheath [2] pointed out that sunscreens used for the protection of human skin against the harmful effects of solar radiation must contain UV-absorbing substances.

Fine particles of various metal oxides, such as ZnO and TiO₂, are extensively used as agents to attenuate (scatter and/or absorb) UV radiation, and have many attractive characteristics, such as a long history of topical use, broad spectrum absorption, high photostability and low irritancy [3]. However, an extensive literature search found that the use of ZnO-TiO₂ as a sunscreen for cosmetic applications has not been fully investigated.

Dulin and Rase [4] first established the basic phase diagram of the ZnO-TiO₂ system, and reported the temperature and composition ranges of stability for zinc metatitanate (ZnTiO₃) and zinc orthotitanate (Zn₂TiO₄). Only Zn₂Ti₃O₈, ZnTiO₃ and Zn₂TiO₄ have been confirmed to exist in ZnO-TiO₂ systems by previous researchers [4–7]. The compound of Zn₂Ti₃O₈ has a cubic structure with a lattice constant of $a_0 = 0.8390(5)$ nm, and has been observed to be a low-temperature form of ZnTiO₃ that exists at temperatures below 820 °C [7]. ZnTiO₃ has a rhombohedral structure with lattice constants of $a_0 = 0.5078(2)$ and $c_0 = 1.3920(1)$ nm [5]. When heated between 965 and 1010 °C, ZnTiO₃ decomposes and forms Zn₂TiO₄ and rutile TiO₂ [6]. The compound of Zn₂TiO₄ has a face-centered cubic crystal structure with a lattice constant of $a_0 = 0.8460(2)$ nm [8].

Zinc titanates, such as ZnTiO₃ and Zn₂TiO₄, are attractive as sorbents for removing sulfur from hot coal gasification products [9,10], pigments [11], and gas sensors for ethanol, NO and CO [12]. Due to the recent progress of microwave applications in the area of mobile telephones and satellite communications, these substances can also be used as dielectric resonators and fitters [13,14]. Furthermore, Chang *et al.* [15,16] also found that doped and undoped ZnTiO₃ have a V-type resistivity-temperature characteristic and possess typical positive thermal coefficient resistivity (PTCR) properties when above the transition point. However, the use of Zn₂Ti₃O₈ or ZnTiO₃ as UV-attenuating agents has not been reported.

The chemistry and microstructure are important factors for applications of zinc titanate powders. Hence, various methods have been adopted for the preparation of ZnTiO₃ powders, including conventional solid state reaction [5] and sol-gel processes [16,17]. In addition, Zn₂TiO₄ powders have been obtained by solid-state reaction [8], and the ball mill method [18]. However, the solid-state reaction processes have some drawbacks, such as high reaction temperature, large particle size and limited degree of chemical homogeneity. On the other hand, Reddy *et al.* [19] pointed out that a single phase of Zn₂Ti₃O₈ is produced when zinc titanyl oxalate hydrate decomposes at 650 °C for several

hours. However, until now, no information is available on the synthesis and characterization of $\text{Zn}_2\text{Ti}_3\text{O}_8$ powders by a hydrothermal process without the addition of a dispersant agent.

In the present study, high purity TiCl_4 and $\text{Zn}(\text{NO}_3)_2 \cdot 6\text{H}_2\text{O}$ have been used for the synthesis of $\text{Zn}_2\text{Ti}_3\text{O}_8$ crystallite powders by a hydrothermal process without the addition of either a dispersant agent or mineralizer. The main purpose of the present investigation was to examine the formation and morphology of $\text{Zn}_2\text{Ti}_3\text{O}_8$ nanocrystallite powders. In addition, this study (i) investigated the thermal behavior of zinc titanate precursor powders, (ii) evaluated the phase transition of zinc titanate precursor powders, and (iii) observed the morphology of zinc titanate precursor powders after calcination at various temperatures for 1 h.

2. Experimental Procedure

2.1. Sample Preparation

The $\text{Zn}_2\text{Ti}_3\text{O}_8$ nanocrystallite powders were prepared by a hydrothermal process without the addition of a dispersant agent. The starting materials were prepared in a aqueous solution with reagent-grade titanium tetrachloride solution (TiCl_4 , purity $\geq 98.0\%$, supplied by Fulka, France), zinc nitrate ($\text{Zn}(\text{NO}_3)_2 \cdot 6\text{H}_2\text{O}$, purity $\geq 98.0\%$, supplied by Alfa Aersor, USA) and 25 vol% ammonia solution (NH_4OH , supplied by Riedel-de Haën, Germany). 0.05 M and 1.0 vol% aqueous solutions were prepared from reagent-grade TiCl_4 , $\text{Zn}(\text{NO}_3)_2 \cdot 6\text{H}_2\text{O}$ and 25 vol% NH_4OH , respectively. A molar ratio of $[\text{Zn}^{2+}]/[\text{Ti}^{4+}]$ was 1.0. An aqueous solution of $\text{Zn}(\text{NO}_3)_2$ was added to TiCl_4 solution under an air atmosphere. The pH of the mixture was then raised to 7.0 by using NH_4OH aqueous solution and stirring the resulting solution for 2 h at room temperature. Subsequently, the solution was kept in an autoclave at 150 °C for 1 h. After cooling, the precipitates obtained were filtered, and washed thoroughly three times with a large amount of deionized water and ethanol (purity $\geq 99.85\%$, supplied by J. J. Baker, USA) to remove Cl^- . The final precipitates were dried at -55 °C in a vacuum and the white zinc titanate precursor powders were thus obtained.

2.2. Sample Characterization

Differential thermal analysis (DTA, Perkin-Elmer 7 Series Thermal Analysis System, Boston, MA, USA) was conducted on 50 mg zinc titanate precursor powders at a heating rate of 10 °C/min in air with a reference material of Al_2O_3 . The calcination temperature was determined from the DTA result.

The crystalline phase was identified using an X-ray diffractometer (XRD, Rigaku D-Max/IIIIV, Tokyo, Japan) with Cu K_α radiation and Ni filter, operated at 30 kV, 20 mA and a scanning rate of 0.25 °/min.

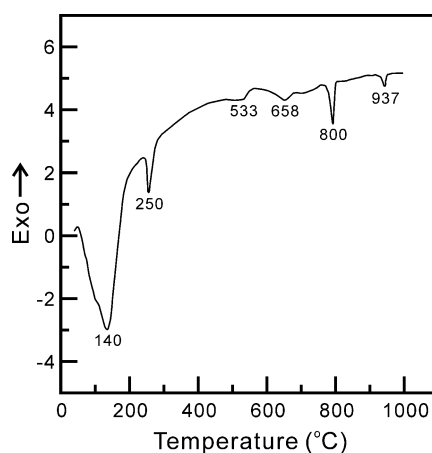
The morphology of the zinc titanate precursor powders calcined at various temperatures for 1 h were observed with a scanning electron microscope (SEM, Hitachi, S-3000N, Japan) and transmission electron microscope (TEM, Hitachi model HF-2000, Tokyo, Japan). The crystal structure of the post-calcined powders was determined by selected area electron diffraction (SAED) analysis. The TEM samples were prepared by dispersing the post-calcined powders in an ultrasonic bath and then collected on a copper grid.

3. Results and Discussion

3.1. Thermal Behavior of the Zinc Titanate Precursor Powders

The DTA curve of the zinc titanate precursor powders, produced without the addition of either a dispersant agent or mineralizer, and which was heated from 25 to 1000 °C in static air at a heating rate of 10 °C/min, is shown in Figure 1. There are four endothermic peaks at 140, 250, 800 and 940 °C in the DTA curve. The endothermic peak at 140 °C is due to the dehydration of the zinc titanate precursor powders. The second endothermic peak, at 250 °C, is attributed to the decomposition of NH_2^- into N_2 and H_2 [20]. The third endothermic peak, at 800 °C, is caused by the decomposition of $\text{Zn}_2\text{Ti}_3\text{O}_8$ into ZnTiO_3 and rutile TiO_2 . The fourth endothermic peak, at 940 °C, is due to the ZnTiO_3 decomposing, which leads to the formation of Zn_2TiO_4 and rutile TiO_2 . Moreover, Figure 1 also shows two relatively small broad exothermic peaks at around 558 and 689 °C. The first exothermic peak, at 558 °C, is due to the anatase TiO_2 accompanied by $\text{Zn}_2\text{Ti}_3\text{O}_8$ formation. The second exothermic peak at 689 °C is caused by the ZnTiO_3 accompanied with rutile TiO_2 formation.

Figure 1. Differential thermal analysis (DTA) curve of zinc titanate precursor powders with a heating rate of $10\text{ }^\circ\text{C}\cdot\text{min}^{-1}$.



3.2. Phase Transition of Zinc Titanate Precursor Powders Calcined at Various Temperatures for 1 h

Figure 2 shows the XRD patterns of the zinc titanate precursor powders prepared without a dispersant agent or mineralizer and calcined at various temperatures for 1 h. The XRD pattern of the freeze dried precursor powders before calcination is shown in Figure 2(a), which reveals that the precursor powders still maintained the amorphous state. Figure 2(b) shows the XRD pattern of the zinc titanate precursor powders calcined at 600 °C for 1 h, and indicates that the anatase TiO_2 appeared due to the reflections located (101), (110), (103), (200), (105), (211) and (220) (JCPDS Cards No.89-4203). Figure 2(b) also shows the presence of ZnO , due to the reflection peaks located at (100), (110) and (103) (JCPDS Card No.89-1397). Furthermore, the reflection peaks of $\text{Zn}_2\text{Ti}_3\text{O}_8$ also appeared at (210), (220), (400), (440), and (622) (JCPDS Card No.87-1991). The XRD pattern of zinc titanate precursor powders calcined at 700 °C for 1 h are illustrated in Figure 2(c), which reveals that the crystallized phases were composed of the major phases of ZnO and $\text{Zn}_2\text{Ti}_3\text{O}_8$, with rutile TiO_2 as the secondary phase and the minor phases of ZnTiO_3 and anatase TiO_2 . Figure 2(d) shows the XRD pattern of zinc

titanate precursor calcined at 900 °C for 1 h. It reveals that the crystallized phase was composed of ZnO, Zn₂TiO₄, rutile TiO₂ and ZnTiO₃, but the anatase TiO₂ disappeared.

Moreover, from Figure 2(c) and (d), it is seen that there is a significantly higher intensity value for the ZnO (100) reflection (I_{100}). Golón *et al.* [21] have pointed out that for hydrothermal treatment systems, samples reveal an apparent preferential orientation growth in the (100) direction, leading to a significant I_{100} value. In fact, zinc and oxygen atoms are arranged alternatively along the c-axis, and thus as is well established, this inherent asymmetry along the c-axis results in the anisotropic growth of ZnO crystallites.

On the other hand, Bartram and Slepetyts [5] pointed out that with a sample prepared at the mole ratio of ZnO:TiO₂ = 2:1 and calcined at 700 and 800 °C for various times, the phase of defect-spinel type Zn₂Ti₃O₈ with a trace amount of uncombined TiO₂ is produced. This is caused by the four Ti ions that are missing from the 16-point positions of the spinel-type structure arrangement, resulting in a defective spinel-type structure. Mrázek *et al.* [22] reported that the TiO₂ and Zn₂TiO₄ are decomposed from prepared Zn_xTi_yO_z powders for various ratios of ZnO/TiO₂. TiO₂ exists at temperatures of 400–600 °C prepared by sol-gel method [23].

In Figure 2(b) and (c), it can be seen that although the intensity of Zn₂Ti₃O₈ increases with the calcination temperature, a small fraction of Zn₂Ti₃O₈ decomposes and leads to the formation of the ZnTiO₃ and rutile TiO₂. This reaction can be expressed as follows:



Yang and Swisher [24] also pointed out that Zn₂Ti₃O₈ is a thermodynamically stable compound up to temperatures between 700 and 800 °C. Just above this temperature, ZnTiO₃ is more stable than the compound of Zn₂Ti₃O₈. Furthermore, Yamaguchi *et al.* [6] also proposed using an amorphous material prepared by the simultaneous hydrolysis of zinc acetylacetonate and titanium isopropoxide for synthesis of the ZnTiO₃ powders. The XRD result shows the reflection peaks of the compound corresponding to Zn₂Ti₃O₈ appeared at 600 °C [5] and the intensity of the reflection peaks increased rapidly up to 760 °C. No other compounds and free species, except for the hexagonal form of ZnTiO₃, are observed up to the decomposition temperature at 965 °C. These results suggest that the compound so far denoted as Zn₂Ti₃O₈ is a low temperature form of ZnTiO₃.

On the other hand, the phase of Zn₂TiO₄ formed by the thermal decomposition of Zn₂Ti₃O₈ in the range of 650–900 °C has been reported by previous studies [5,25]. Figure 2(c) shows that for the zinc titanate precursor powders calcined at 700 °C for 1 h, only a small fraction of Zn₂Ti₃O₈ decomposed and formed the ZnTiO₃ and rutile TiO₂. This result was attributed to the fact that the phase of Zn₂Ti₃O₈ at 700 °C still has thermal stability. When calcined at 900 °C for 1 h, the Zn₂Ti₃O₈ phase disappeared and the reflection peaks of ZnTiO₃ also nearly vanished, but the intensity of Zn₂TiO₄ and rutile TiO₂ increased. This is because the Zn₂Ti₃O₈ and ZnTiO₃ phases decomposed, leading to the formation of Zn₂TiO₄ and rutile TiO₂. These reactions can be expressed as follows:

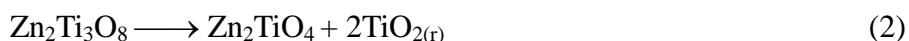
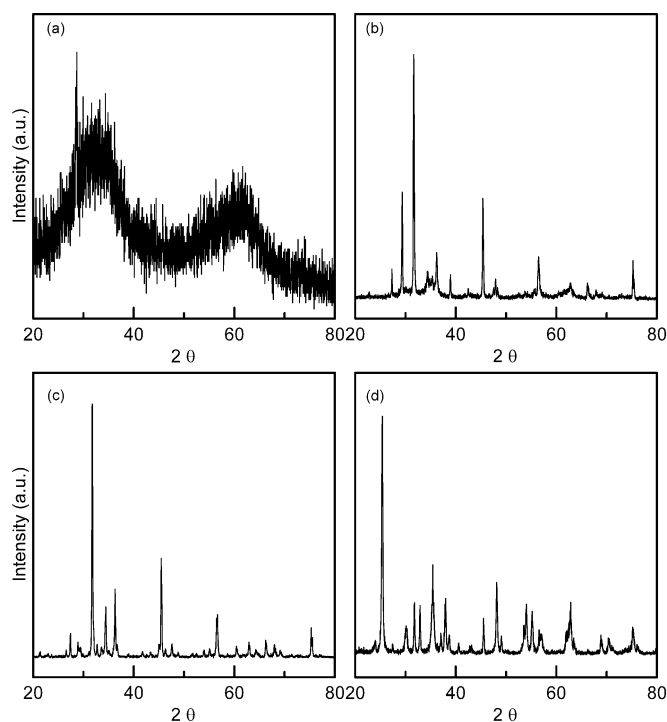


Figure 2. X-ray diffraction (XRD) patterns of ZnTiO_3 precipitates calcined at various temperatures for 1 h: (a) before calcination, (b) calcined at 600 °C, (c) 700 °C, and (d) 900 °C.



3.3. Microstructure of the Zinc Titanate Precursor Powders Calcined at Various Temperatures for 1 h

The SEM microstructure of the zinc titanate precursor powders calcined at various temperatures for 1 h are shown in Figure 3. Figure 3(a) shows the morphology of the freeze-dried zinc titanate precursor powders without a dispersant agent or mineralizer agglomerates to the size of about $140 \pm 70 \mu\text{m}$. The SEM micrographs in Figure 3(b) and (d) shows the zinc titanate precursor powders calcined at 600, 700 and 900 °C for 1 h, respectively. It can be seen that the agglomerated size of the particles increases as the calcination temperature rises from 600 to 900 °C. When calcined at 900 °C for 1 h, the size increases from $140 \pm 70 \mu\text{m}$ to $270 \pm 170 \mu\text{m}$. Since the zinc titanate precursor powders were prepared through the wet-chemical routes, during this process, *i.e.*, drying and/or subsequent steps, agglomeration can occur. During calcination, the most common type of agglomeration in the conventional powders was due to solid bonds that formed between the particles.

The bright field (BF) and dark field (DF) TEM micrographs and the corresponding electron diffraction (ED) patterns of the freeze dried zinc titanate precursor powders calcined at 700 °C for 1 h are shown in Figure 4. Figure 4(a) shows the BF image, in which fine particles with size of about 5 nm and a larger particle with a length of 200 nm and width of 100 nm are observed. Aubert *et al.* [26] also reported the particle of TiO_2 is about 5 nm. Figure 4(a) shows that the larger particles, of ZnO which cause the contact area of ZnO with anatase TiO_2 to decrease, led to a decrease in the reaction of ZnO with anatase TiO_2 , meaning that insufficient $\text{Zn}_2\text{Ti}_3\text{O}_8$ was produced. Figure 4(b),(c) shows the DF images of the fine and larger particles in Figure 4(a). In addition, Figure 4(d),(e) shows the ED patterns of the particles in Figure 3(b),(c), respectively. The ED pattern of Figure 4(d) corresponds to the phases of ZnTiO_3 and rutile TiO_2 . On the other hand, the ED pattern of Figure 4(e) corresponds to ZnO.

Figure 4(d) also shows evidence of ZnTiO_3 and rutile TiO_2 when calcined at $700\text{ }^\circ\text{C}$ for 1 h. Moreover, the microstructure of the ZnTiO_3 crystallite shows a nearly spherical morphology growing on the matrix of a plate-like phase of ZnO .

Figure 3. Scanning electron microscope (SEM) morphology of zinc titanate precursor powders calcined at various temperatures for 1 h: (a) before calcination, (b) calcined at $600\text{ }^\circ\text{C}$, (c) $700\text{ }^\circ\text{C}$, and (d) $900\text{ }^\circ\text{C}$.

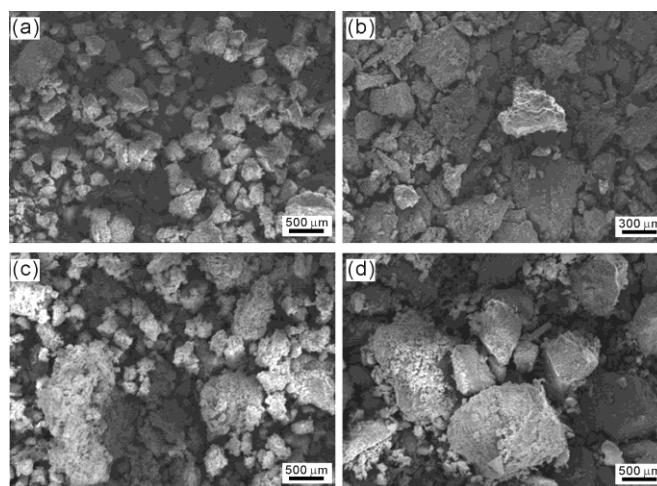


Figure 4. Transmission electron microscope (TEM) morphology and electron diffraction (ED) patterns of zinc titanate precursor powders calcined at $700\text{ }^\circ\text{C}$ for 1 h: (a) bright field (BF) image, (b) dark field (DF) image by using a circle spot of (d), (c) DF image by using a circle spot of (e), (d) ED pattern corresponding to the phases of $\text{Zn}_2\text{Ti}_3\text{O}_8$ (denoted by ZT) and rutile TiO_2 (denoted by r), and (e) ED pattern corresponding to ZnO .

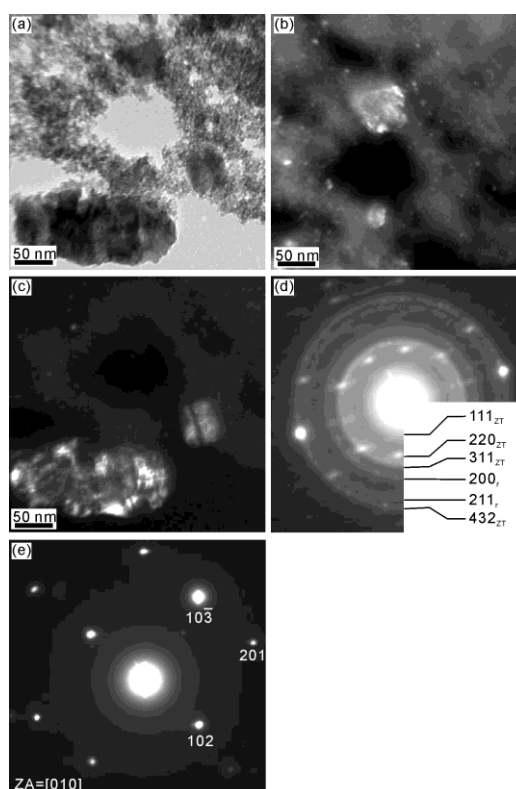
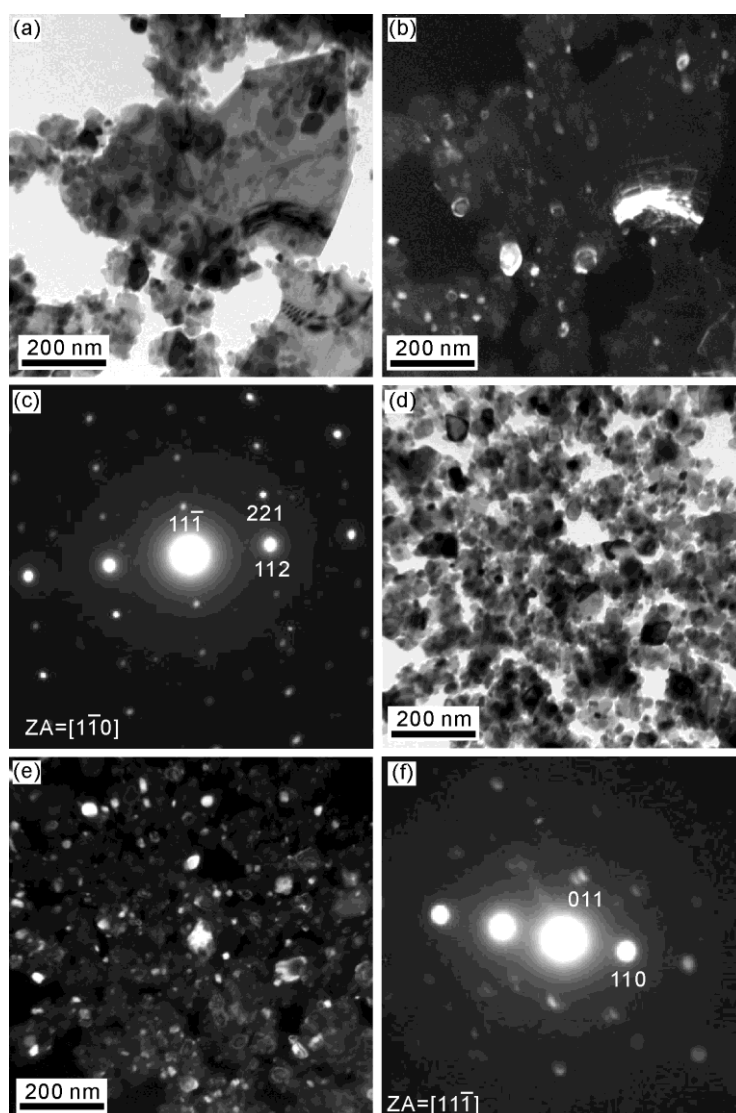


Figure 5(a),(b) shows the BF and DF images of the freeze dried zinc titanate precursor powders calcined at 900°C for 1 h, revealing that two kinds morphology coexist in the sample. One is the fine particles with a size of about 50 nm, and the other one is belt-shape particles with a length of 200 nm and width of 50 nm. The ED pattern of the Figure 5(c) belt-shaped and fine particles correspond to ZnTiO_3 with a zone axis (ZA) of $[110]$. Figure 5(d),(e) shows the BF and DF images of the fine particles with the size of about $38 \pm 18 \text{ nm}$. The ED pattern of Figure 5(f) corresponds to Zn_2TiO_3 with the ZA of $[\bar{1}\bar{1}\bar{1}]$.

Figure 5. TEM morphology and ED patterns of zinc titanate precursor powders calcined at 900 °C for 1 h: (a) BF image, (b) DF image by using a circle spot of (c), (c) ED pattern corresponding to ZnTiO_3 , (d) BF image, (e) DF image by using a circle spot of (f), and (f) ED pattern corresponding to Zn_2TiO_3 .

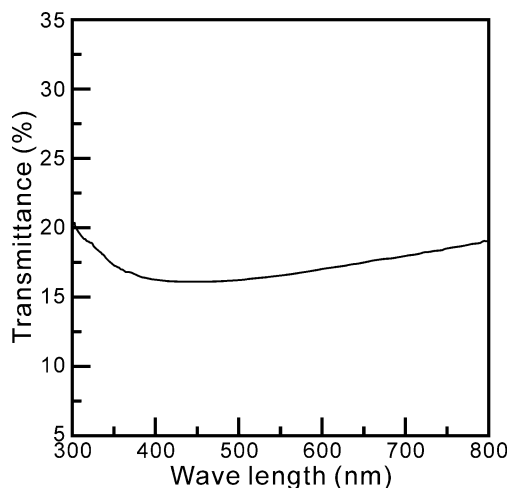


3.4. The Transmittance of Zinc Titanate Precursor Powders Calcined at 900 °C for 1 h

Figure 6 shows the relation between transmittance and wavelength range between 300 and 800 nm for freeze dried zinc precursor powders calcined at 700 °C for 1 h. It is found that the calcined sample

has an acceptable transmittance at the wavelength of 400 nm. This result indicates that zinc titanate precursor powders calcined at 700 °C for 1 h can be used as an UVA-attenuating agent.

Figure 6. Relation between the absorbed and wavelength between 300 and 800 nm for ZnTiO₃ precipitates calcined at 900 °C for 1 h.



4. Conclusions

Zn₂Ti₃O₈ powders prepared by a hydrothermal method without a dispersant agent or mineralizer for use in UVA-attenuating applications have been investigated using DTA, XRD, SEM, TEM, ED and UV/VIS. The results are summarized as follows:

- (1) When the zinc titanate precursor powders were prepared at pH = 7 and calcined at 600 °C for 1 h, the XRD results show that the phases of ZnO, anatase TiO₂ and Zn₂Ti₃O₈ coexisted in the sample. However, when calcined at 900 °C for 1 h, the XRD result reveals the existence of Zn₂TiO₄, rutile TiO₂, and ZnO.
- (2) The SEM results reveal significant agglomeration in both the freeze-dried and post-calcined samples.
- (3) The TEM and ED examination indicates the existence of near spherical Zn₂Ti₃O₈ crystallites with size of about 5 nm on larger ZnO particles with a length of 200 nm and width of 100 nm. The microstructure ZnTiO₃ shows a somewhat belt-shaped morphology, with a length of 200 nm and width of 50 nm for precipitates calcined at 900 °C for 1 h.
- (4) The calcined samples have an acceptable transmittance when the wavelength is 400 nm. This result indicates that zinc titanate precursor powders calcined at 700 °C for 1 h can be used as an UVA-attenuating agent.

Acknowledgments

This work was supported by the National Science Council and Kaohsiung Medical University, Taiwan, under Contract No.95-2221-E-037-007 and Q 097038, respectively, which is gratefully acknowledged. In addition, the authors sincerely thank M.P Hung and M.H. Hon for the discussions and S.Y. Yau for the assistance in TEM.

References

1. Fairhurst, D.; Mitchnick, M.A. In *Sunscreens: Development, Evaluation, and Regulatory Aspects*, 2nd ed.; Lowe, N.J., Shaath, N.A., Pathat, M.A., Eds.; Marcel Dekker: New York, NY, USA, 1997; pp. 313–352.
2. Shaath, N.A. *Sunscreens: Development, Evaluation, and Regulatory Aspects*, 2nd ed.; Lowe, N.J., Shaath, N.A., Pathat, M.A., Eds.; Marcel Dekker: New York, NY, USA, 1997; pp. 3–33.
3. Al-Hill, S.M.; Willamder, M. Optical properties of zinc oxide nano-particles embedded in dielectric medium for UV region: Numerical simulation. *J. Nanoparticle Res.* **2006**, *8*, 79–97.
4. Dulin, F.H.; Rase, D.E. Phase equilibria in the system ZnO-TiO₂. *J. Am. Ceram. Soc.* **1960**, *43*, 125–131.
5. Bartram, S.F.; Slepety, R.A. Compound formation and crystal structure in the system ZnO-TiO₂. *J. Am. Ceram. Soc.* **1961**, *44*, 493–499.
6. Yamaguchi, O.; Morimi, M.; Kawabata, H.; Shimizu, K. Formation and transformation of ZnTiO₃. *J. Am. Ceram. Soc.* **1987**, *70*, 97–98.
7. Steinike, U.; Wallis, B. Formation and Structure of Ti-Zn-Oxides. *Cryst. Res. Technol.* **1997**, *32*, 187–193.
8. Kim, H.T.; Kim, Y.; Valant, M.; Suvorov, D. Titanium incorporation in Zn₂TiO₄ spinel ceramics. *J. Am. Ceram. Soc.* **2001**, *84*, 1081–1086.
9. Swisher, J.H.; Schwerdtfeger, K. Thermodynamic analysis of sorption reactions for the removal of sulfur from hot gases. *J. Mater. Eng. Preform.* **1992**, *1*, 565–571.
10. Swisher, J.H.; Yang, J.; Gupta, R.P. Attrition-resistant zinc titanate sorbent for Sulfur. *Ind. Eng. Chem.* **1995**, *34*, 4463–4471.
11. McCord, A.T.; Saunderson, H.F. Preparation of pigmentary materials. US Patent 2379019, 1945.
12. Obayashi, H.; Sakurai, Y.; Gejo, T. Perovskite-type oxide as ethanol sensors. *J. Solid State Chem.* **1976**, *17*, 299–303.
13. Kagata, H.; Inoue, T.; Kato, J.; Kameyama, I.; Ishizaki, T. Low-fire microwave dielectric ceramics, and multilayer devices with silver internal electrode. *Ceram. Trans.* **1993**, *32*, 81–90.
14. Negas, T.; Yeager, T.; Bell, S.; Coats, N.; Minis, I. BaTi₉O₂₀-based ceramics resulted for modern microwave applications. *Am. Ceram. Soc. Bull.* **1993**, *72*, 80–89.
15. Chang, Y.S.; Chang, Y.H.; Chen, I.G.; Chen, G.J. Synthesis and characterization of zinc titanate doped with magnesium. *Solid State Commun.* **2003**, *128*, 203–208.
16. Chang, Y.S.; Chang, Y.H.; Chen, I.G.; Chen, G.J.; Chai, Y.L. Synthesis and characterization of zinc titanate nano-crystal powders by sol-gel technique. *J. Cryst. Growth* **2002**, *243*, 319–326.
17. Hosono, E.; Fujihara, S.; Onuki, M.; Kimura, T. Low-temperature synthesis of nanocrystalline zinc titanate materials with high specific surface area. *J. Am. Ceram. Soc.* **2004**, *87*, 1785–1788.
18. Manik, S.K.; Bose, P.; Pradhan, S.K. Microstructure characterization and phase transformation kinetics of ball-milled prepared nanocrystalline Zn₂TiO₄ by Rietveld method. *Mater. Chem. Phys.* **2003**, *82*, 837–847.
19. Reddy, V.B.; Goel, S.P.; Mehrotra, P.N. Investigation on formation of zinc titanates via thermal decomposition of zinc titanyl oxalate hydrate. *Mater. Chem. Phys.* **1984**, *10*, 365–373.

20. Kuo, C.L.; Wang, C.L.; Chen, T.Y.; Chen, G.J.; Hung, I.M.; Shih, C.J.; Fung, K.Z. Low-temperature synthesis of nanocrystalline lanthanum monoaluminate powders by chemical co-precipitation. *J. Alloy. Compd.* **2007**, *392*, 367–374.
21. Golón, G.; Hidalgo, M.C.; Navó, J.A.; Melián, E.P.; Dáz, O.G.; Rodriguez, J.M.D. Highly photoactive ZnO by amine capping-assisted hydrothermal treatment. *Appl. Catal. B Environ.* **2008**, *83*, 30–38.
22. Krylova, G.; Brioude, A.; Girard, S.A.; Mrazek, J.; Spanhel, L. Natural superhydrophilicity and photocatalytic properties of sol-gel derived ZnTiO₃-ilmenite/r-TiO₂ films. *Phys. Chem. Chem. Phys.* **2010**, *12*, 15101–15110.
23. Aubert, T.; Grasset, F.; Potel, M.; Nazabal, V.; Cardinal, T.; Pechev, S.; Saito, N.; Ohashi, N.; Haneda, H. Synthesis and characterization of Eu³⁺,Ti⁴⁺@ZnO organosols and nanocrystalline c-ZnTiO₃ thin films aiming at high transparency and luminescence. *Sci. Technol. Adv. Mater.* **2010**, *11*, 044401.
24. Yang, J.; Swisher, J.H. The phase stability of Zn₂Ti₃O₈. *Mater. Character.* **1996**, *37*, 153–159.
25. Aal, A.A.; Barakat, M.A.; Mohamed, R.M. Electrophoreted Zn-TiO₂-ZnO nanocomposite coating films for photocatalytic degradation of 2-chlorophenol. *Appl. Surface Sci.* **2008**, *254*, 4577–4583.
26. Mrázek, J.; Spanhel, L.; Chadeyron, G.; Matějec, V. Evolution and Eu³⁺ doping of sol-gel derived ternary Zn_xTi_yO_z nanocrystals. *J. Phys. Chem. C* **2010**, *114*, 2843–2852.

© 2011 by the authors; licensee MDPI, Basel, Switzerland. This article is an open access article distributed under the terms and conditions of the Creative Commons Attribution license (<http://creativecommons.org/licenses/by/3.0/>).